

Analytically exact solution of the Schrödinger equation for neutral helium in the ground state

by Frank Kowol, May 2024

1. Abstract

This report presents the analytical solution of the Schrodinger equation and its corresponding wave function for the neutral helium or helium-like atoms in the ground state. The state functions of the two electrons for $s=0$ and $l=0$ as well as their boundary conditions are examined in detail. Furthermore, a method for describing a generic electron potential consisting of Coulomb and exchange interactions is derived, and the resulting potential function is integrated into the Schrodinger equation as a potential term. In addition, the altered electromagnetic coupling of the electrons due to vacuum polarization effects is investigated and finally the Schrodinger equation for the neutral $1s^2 \ ^1S_0$ Helium, historically known as Para-Helium, is solved using Laplace transformations. The energy in the ground state is then determined, and it can be shown that this agrees with the literature values given the fact that the electron can be assumed to be a point-like particle. In the context of these investigations, an upper limit estimation for the spatial dimension of the electron can also be given as well as the existence of a minimal distance of a stable bonding state between two electrons, which can be interpreted as an entangled state; in addition, the chemical inertness of helium with regard to chemical reactions - i.e. the principle of the "closed" electron shell - can be made plausible by the quantum mechanical electron configuration and its consequences with regard to binding energy. The wave function found for the helium atom is compared with the known solutions for the hydrogen atom, and essential differences between the two are worked out.

2. Basic prerequisites and motivation

The neutral helium atom is one of the trickiest problems in modern physics, as it combines the supposedly simple and already well-understood structure of a quantum-mechanical hydrogen-like system with well-defined quantum numbers with the problem of a three-body problem. Since the work of Hylleraas in 1930 [1], many attempts have been made to solve the Schrödinger equation, numerical approaches and variation calculus with great success over the years [2-16]. In 2006, for example, the calculations could now be calculated with an accuracy of 35 decimal places [17]. However, a non-analytical approach has the disadvantage that the basic mechanisms of action that ultimately lead to the binding energy remain opaque. A real understanding of the helium atom, its energy configuration in the ground state and the mechanism of a closed shell remain in the dark. An analytical solution is therefore to be preferred in any case, but so far it has not been possible to realize it despite many attempts with various approaches and different wave functions [11-16]. This is mainly caused by a three-body problem of a nucleon-electron-electron configuration that results in a non-linear Schrödinger equation and such cannot be solved trivially without further ado. In addition, there is the question of the exact configuration of the two electrons. The idea of a quasi-planetary system with two planets - the electrons - and a sun - the nucleus - is just as misleading as the idea of an arbitrarily diffuse wave function, especially since the system in the ground state of a $1s^2 \ ^1S_0$ - helium configuration has neither an orbital angular momentum nor a net total electron spin. It is easy to see that a multipole moment would always arise in the particle picture with two separately localized electrons and a nucleus, especially if one assumed configurations of minimum energy in which the electrons would occupy quasi-opposite positions. However, such a multipole moment, regardless of the type, has never been observed [3,9,11,14] and is also prohibited by quantum mechanics in the $1S$ singlet state. To derive a valid analytical solution, a few steps are now required, which are discussed in the following sections:

- First, the nature of the ground state for the electrons is examined in more detail. It can be shown here that the electrons occupy the same identical state.
- The next step is to access a general formulation for the electric potential, or the exchange interaction of the electron. The decisive difference between the hydrogen and helium configurations - apart from the obvious fact of the double nuclear charge - is the presence of a second electron, which has a decisive influence on the potential terms and thus on the wave functions and its binding energy.
- Even with complete consideration of both electrons and the nucleus, deviations still occur in the form of an increased coupling factor between the two electrons. This section looks at the cause of

the coupling and its fascinating consequences and determines the correction factor to reproduce the correct binding energy.

- With the preliminary work, an analytical solution of the Schrodinger equation can now be worked out. The Laplace transformation method is used for this. This is followed by a comparison of the wave function of hydrogen with the wave function of helium derived in this report to develop an understanding of the influence of the multi-electron configuration.
- Finally, the analysis of the energy in the ground state can be performed. However, due to the special nature of helium, only the ground state is analyzed in more detail rather than the energy spectrum.
- Summary and outlook as well as the bibliography and the documentation of the MATLAB code used finally round off this report.

3. Identical electronic states in the 1S_0 Helium

As mentioned above, the electron states of helium in the ground state are of particular interest. Quantum systems of this type are already very well understood in the literature [9-14]. Thus, the well-defined quantum numbers n, l and s can also be used here to describe the orbital states. To simplify matters, $n = 1, l = 0, s = 0$ is used here, i.e., helium in the ground state, because this system already offers sufficient complexity for a deeper description. If we now look at the electron states, we must show that both electrons have identical wave functions with antiparallel spin functions and symmetrical local wave functions, provided the energy values are not degenerated.

In other words, it must be shown that two S-electrons with antiparallel spin and a radially symmetric wave function in a central potential without an external field have identical energy levels if they have identical wave functions.

To proof this now, consider the expectation value for a two-particle system of fermions, here specifically electrons. Then the expectation value of an operator \hat{O} is composed of the direct Coulomb term C and the exchange term A .

$$\langle \Psi(\vec{r}_1, \vec{r}_2) | \hat{O} | \Psi(\vec{r}_1, \vec{r}_2) \rangle = C \pm A$$

$$\Leftrightarrow \langle \Psi(\vec{r}_1, \vec{r}_2) | \hat{O} | \Psi(\vec{r}_1, \vec{r}_2) \rangle = \frac{1}{\sqrt{2}} \langle \phi(\vec{r}_1) \psi(\vec{r}_2) | \hat{O} | \phi(\vec{r}_1) \psi(\vec{r}_2) \rangle \pm \frac{1}{\sqrt{2}} \langle \psi(\vec{r}_1) \phi(\vec{r}_2) | \hat{O} | \phi(\vec{r}_1) \psi(\vec{r}_2) \rangle$$

This leads to the well-known splitting of the helium into the “ortho” state with parallel spins and the “para” state with antiparallel spins. If we consider the $1s^2$ 1S_0 state with its energy singlet state, i.e., there is only one observable energy state for the two-particle electron system with electrons i and j . The two-particle wave function, consisting of the partial wave functions ψ and ϕ , behaves antisymmetrically with respect to interchange, i.e., with antiparallel spin functions the local wave function of both electrons must be symmetrical:

$$\Psi(\vec{r}_j, \vec{r}_i) = \Psi(\vec{r}_i, \vec{r}_j) \Leftrightarrow \phi(\vec{r}_i)\psi(\vec{r}_j) = \psi(\vec{r}_j)\phi(\vec{r}_i)$$

With the normalization condition

$$\langle \psi(\vec{r}_i) | \psi(\vec{r}_i) \rangle = \langle \phi(\vec{r}_i) | \phi(\vec{r}_i) \rangle = \langle \psi(\vec{r}_j) | \psi(\vec{r}_j) \rangle = \langle \phi(\vec{r}_j) | \phi(\vec{r}_j) \rangle = 1$$

So, the following expression must apply with the identity for the dyadic product: $|\psi(\vec{r}_i)\rangle\langle\psi(\vec{r}_i)| = |\phi(\vec{r}_i)\rangle\langle\phi(\vec{r}_i)| = \mathbb{I}$:

$$\langle \phi(\vec{r}_i) | \psi(\vec{r}_j) \rangle = \langle \psi(\vec{r}_i) | \phi(\vec{r}_j) \rangle \quad (1)$$

$$\begin{aligned} \langle \phi(\vec{r}_i) | \psi(\vec{r}_i) \rangle \langle \psi(\vec{r}_i) | \psi(\vec{r}_j) \rangle &= \langle \psi(\vec{r}_i) | \psi(\vec{r}_j) \rangle \langle \psi(\vec{r}_j) | \phi(\vec{r}_j) \rangle \\ \Leftrightarrow \langle \phi(\vec{r}_i) | \psi(\vec{r}_i) \rangle &= \langle \psi(\vec{r}_j) | \phi(\vec{r}_j) \rangle \end{aligned} \quad (2)$$

As well as:

$$\begin{aligned} \langle \phi(\vec{r}_i) | \phi(\vec{r}_j) \rangle \langle \phi(\vec{r}_j) | \psi(\vec{r}_j) \rangle &= \langle \psi(\vec{r}_i) | \phi(\vec{r}_i) \rangle \langle \phi(\vec{r}_i) | \phi(\vec{r}_j) \rangle \\ \Leftrightarrow \langle \phi(\vec{r}_j) | \psi(\vec{r}_j) \rangle &= \langle \psi(\vec{r}_i) | \phi(\vec{r}_i) \rangle \end{aligned} \quad (3)$$

Whereas the term was divided by $\langle \psi(\vec{r}_i) | \psi(\vec{r}_j) \rangle \neq 0$, resp. $\langle \phi(\vec{r}_i) | \phi(\vec{r}_j) \rangle \neq 0$. The transition probabilities are not equal to 0 due to the exchange interaction. Now let the three identities be used and multiplied from the right and left, respectively:

$$\begin{aligned} \langle \psi(\vec{r}_i) | \phi(\vec{r}_i) \rangle \langle \phi(\vec{r}_i) | \psi(\vec{r}_j) \rangle \langle \psi(\vec{r}_j) | \phi(\vec{r}_j) \rangle &= \langle \phi(\vec{r}_j) | \psi(\vec{r}_j) \rangle \langle \psi(\vec{r}_i) | \phi(\vec{r}_j) \rangle \langle \phi(\vec{r}_i) | \psi(\vec{r}_i) \rangle \\ \Leftrightarrow \langle \psi(\vec{r}_i) | \phi(\vec{r}_j) \rangle &= \langle \phi(\vec{r}_j) | \psi(\vec{r}_j) \rangle \langle \psi(\vec{r}_i) | \phi(\vec{r}_j) \rangle \langle \phi(\vec{r}_i) | \psi(\vec{r}_i) \rangle \end{aligned}$$

So, by using the dyadic product and dividing $\langle \psi(\vec{r}_i) | \phi(\vec{r}_j) \rangle \neq 0$ (the exchange interaction also applies here), the result is given by (4):

$$\Leftrightarrow \mathbb{I} = \langle \phi(\vec{r}_j) | \psi(\vec{r}_j) \rangle \langle \phi(\vec{r}_i) | \psi(\vec{r}_i) \rangle \quad (4)$$

This can only apply if the transition amplitude of both wave functions = 1, i.e., the indistinguishable electrons can freely pass over to the other wave function. This means that both quantum states are interchangeable and both wave functions should be identical at the same energy level $\psi(\vec{r}) = \phi(\vec{r})$. If this is followed up, it is to be shown that for identical energy states in a rotationally symmetric potential, the wave functions must also be identical, provided the spatial function is symmetric. Then let E_1 for $\psi(\vec{r})$ and E_2 for $\phi(\vec{r})$ apply to their binding energies:

$$\Delta E = E_1 - E_2 = 0$$

Now the Schrodinger equation is to be considered and compared with the Hamilton operator for both electrons. In particular, the wave function in the charge field of the other electron should also be considered, provided this is also rotationally symmetric. This must be the case, as the ground state with $l, s = 0$ is still considered. If we now set up both Schrodinger equations for the wave functions of the respective electrons, the following applies:

$$0 = E_1 - E_2 = \langle \psi | \hat{H}_1 | \psi \rangle - \langle \phi | \hat{H}_2 | \phi \rangle \quad (5)$$

With the formula for \hat{H} for $\psi(r)$ and $\phi(r)$ the following term applies:

$$\int_0^\infty r^2 \psi^*(r) \left(\frac{\partial^2}{\partial r^2} \psi(r) + \frac{2}{r} \frac{\partial}{\partial r} \psi(r) + V(r) \psi(r) \right) dr = E_1$$

$$\int_0^\infty r^2 \phi^*(r) \left(\frac{\partial^2}{\partial r^2} \phi(r) + \frac{2}{r} \frac{\partial}{\partial r} \phi(r) + V(r) \phi(r) \right) dr = E_2$$

If one forms the difference according to (5):

$$\begin{aligned}
&\Leftrightarrow \int_0^\infty r^2 \psi^* \left(\frac{\partial^2}{\partial r^2} \psi + \frac{2}{r} \frac{\partial}{\partial r} \psi + V(r) \psi \right) dr - \int_0^\infty r^2 \phi^* \left(\frac{\partial^2}{\partial r^2} \phi + \frac{2}{r} \frac{\partial}{\partial r} \phi + V(r) \phi \right) dr = 0 \\
&\Leftrightarrow \int_0^\infty r^2 \left(\psi^* \frac{\partial^2}{\partial r^2} \psi - \phi^* \frac{\partial^2}{\partial r^2} \phi \right) dr + \int_0^\infty r^2 \frac{2}{r} \left(\psi^* \frac{\partial}{\partial r} \psi - \phi^* \frac{\partial}{\partial r} \phi \right) dr + \int_0^\infty r^2 (\psi^* V(r) \psi - \phi^* V(r) \phi) dr = 0 \\
&\Leftrightarrow \int_0^\infty r^2 \left(\psi^* \frac{\partial^2}{\partial r^2} \psi - \phi^* \frac{\partial^2}{\partial r^2} \phi \right) dr + \int_0^\infty 2r \left(\psi^* \frac{\partial}{\partial r} \psi - \phi^* \frac{\partial}{\partial r} \phi \right) dr + \int_0^\infty r^2 V(r) (|\psi|^2 - |\phi|^2) dr = 0
\end{aligned}$$

Now note further from (1) that the two electrons can exchange places freely due to the exchange interaction effect, provided that the energy condition is observed according to Fermi's golden rule:

$$|c_{\psi,\phi}(t)|^2 = \frac{2t}{\hbar} \pi |\langle \psi | \hat{\mathcal{M}} | \phi \rangle|^2 \delta(E_1 - E_2) \text{ with } \hat{\mathcal{M}} = \mathbb{I}$$

In the experiment, only the singlet state with one energy level is found for the ground state of helium, $E_1 = E_2$ therefore applies. The Schrodinger equation then follows from the permutation and from (4):

$$\Leftrightarrow \int_0^\infty r^2 \left(\psi^* \frac{\partial^2}{\partial r^2} \psi - \phi^* \frac{\partial^2}{\partial r^2} \phi \right) dr + \int_0^\infty 2r \left(\psi^* \frac{\partial}{\partial r} \psi - \phi^* \frac{\partial}{\partial r} \phi \right) dr + \int_0^\infty r^2 V(r) (|\psi|^2 - |\phi|^2) dr = 0$$

1.) 2.) 3.)

$$1.) \psi^* \frac{\partial^2}{\partial r^2} \psi - \phi^* \frac{\partial^2}{\partial r^2} \phi = \phi^* \frac{\partial^2}{\partial r^2} \phi - \psi^* \frac{\partial^2}{\partial r^2} \psi \Leftrightarrow \psi^* \frac{\partial^2}{\partial r^2} \psi = \phi^* \frac{\partial^2}{\partial r^2} \phi$$

$$2.) \psi^* \frac{\partial}{\partial r} \psi - \phi^* \frac{\partial}{\partial r} \phi = \phi^* \frac{\partial}{\partial r} \phi - \psi^* \frac{\partial}{\partial r} \psi \Leftrightarrow \psi^* \frac{\partial}{\partial r} \psi = \phi^* \frac{\partial}{\partial r} \phi$$

$$3.) |\psi|^2 - |\phi|^2 = |\phi|^2 - |\psi|^2 \Leftrightarrow |\psi|^2 = |\phi|^2$$

Now one applies 3.) and multiplies from the left side $\phi\psi$, while $\phi, \psi \neq 0 \forall r$. This means that:

$$\phi\psi\psi^* \frac{d}{dr}\psi = \phi\psi\phi^* \frac{d}{dr}\phi \Leftrightarrow \phi|\psi|^2 \frac{d}{dr}\psi = \psi|\phi|^2 \frac{d}{dr}\phi \stackrel{\text{mit 3.}}{\Leftrightarrow} \frac{1}{\psi} \frac{d}{dr}\psi = \frac{1}{\phi} \frac{d}{dr}\phi$$

$$\Leftrightarrow \frac{1}{\psi} \frac{d}{dr} \psi = \frac{1}{\phi} \frac{d}{dr} \phi \xrightarrow{\text{Integration}} \ln \psi = \ln \phi \Leftrightarrow \psi = \phi \quad q.e.d.$$

Thus, it follows that in a central potential, the rotationally symmetric state functions for electrons with zero angular momentum and zero spin are identical if their energy levels are identical. This provides the basis for further work: Both electrons are in the exact same state function without polarization, without multipole momentum and without being distinguishable. This turns out to be an essential feature for solving the Schrodinger equation later in this report.

4. Derivation of the general electron potential

To correctly reflect the mutual effect of the electrons on each other, the electron wave function must be made usable in generalized form as a potential term. The square of the electron wave functions $\psi^*\psi$, $\phi^*\phi$ can simultaneously be interpreted as a charge cloud and thus fits into the overall potential in helium. At the same time, however, the exchange integrals $\psi^*\phi$ and $\phi^*\psi$ can also be interpreted as potential terms. This is particularly important because such potential terms must be generically evaluable for a differential equation such as the Schrödinger equation to ultimately derive valid solutions of the wave functions. To approach in an adequate way, the general approach is therefore defined as a sum of arbitrary wave functions:

$$\psi^*(r)\chi(r) = \sum_n A_n r^n e^{-a_n r} \quad A_n \in \mathbb{R}, a_n > 0 \quad (6)$$

ψ and χ can, but need not be identical to cover both the Coulomb- and the exchange term as well. Let it now be given that ψ and ϕ are square-integrable and normalizable, and that $|\psi(r)|^2 > 0$ and $|\chi(r)|^2 > 0$ applies to whole \mathbb{R}_0^+ . Then, based on the solutions of the hydrogen atom, a general wave function can be specified as the sum of decreasing exponential functions multiplied by a polynomial as defined in (6). This also applies to composite functions or fractions, because either the representation can be generated via partial fraction decomposition and splitting of the fractions, or the series expansions can be used to find a suitable summation.

A well-known approach from electrodynamics is now used, in which the effective total potential can be calculated using the convolution product of a charge distribution with a given point charge potential [18-20]. Consider a distributed charge:

$$\phi(\vec{r}) = \frac{1}{4\pi\epsilon_0} \int \frac{\rho(\vec{r}')}{|\vec{r} - \vec{r}'|} d\vec{r}'$$

Respectively for the given case of radial symmetric charge distributions:

$$\phi(r) = \frac{1}{4\pi\epsilon_0} \int \frac{\rho(r')}{|r - r'|} dr'$$

This expression can then also be interpreted as a convolution between a charge density and the potential function. It may be explicitly stated that (6) is interpreted formally as a charge density. One will later see that this is the case in the He-ground state. This also means that the convolution can be formed as an inverse Fourier transform from the multiplication of the two Fourier transforms according to the integration theorem [20]:

$$[f \otimes g](r) = \int_{\mathbb{R}} f(r') g(r - r') dr' = \frac{1}{\sqrt{2\pi}^3} \mathcal{F}^{-1}[\mathcal{F}(f(r)) \cdot \mathcal{F}(g(r))](r) \quad (7)$$

While the definitions of charge density and the potential of the point charge the following equation are given:

$$f(r) \equiv \rho(r) \text{ and } g(r) \equiv \phi_e(r) = \frac{1}{4\pi\epsilon_0} \frac{1}{|r - r'|}$$

And the Fourier Transform respectively:

$$\mathcal{F}(\phi_e(r))(\omega) = \mathcal{F}\left(\frac{1}{4\pi\epsilon_0} \frac{1}{|r|}\right)(\omega) = \frac{1}{4\pi\epsilon_0} i \sqrt{\frac{\pi}{2}} sgn(\omega)$$

$$\mathcal{F}(\rho(r))(\omega) = e\mathcal{F}(r^2|R(r)|^2)(\omega)$$

If we now apply the general formulation for a charge distribution from (6), the expression can be converted into a Fourier transform:

$$\mathcal{F}\left(\sum_n A_n r^n e^{-a_n r}\right)(\omega) = \frac{1}{\sqrt{2\pi}} \sum_n \frac{A_n n!}{(a_n + i\omega)^{n+1}} \text{ mit } A_n, a_n \in \mathbb{R}, a_n > 0 \quad (8)$$

If (8) is combined with the Fourier transform of the potential, the result is:

$$\phi(r) = \frac{1}{\sqrt{2\pi}^3} \frac{e}{4\pi\epsilon_0} \mathcal{F}^{-1}\left\{\mathcal{F}\left(\frac{1}{4\pi\epsilon_0} \frac{1}{|r|}\right) \cdot \mathcal{F}\left(\sum_n A_n r^n e^{-a_n r}\right)\right\}(r)$$

This leads to the fully formulated integral:

$$\begin{aligned} \phi(r) &= \frac{1}{2\sqrt{2\pi}} \frac{e}{4\pi\epsilon_0} \sum_n \int_{-\infty}^{\infty} \frac{i A_n n! sgn(\omega) e^{i\omega r}}{(a_n + i\omega)^{n+1}} d\omega \\ \Leftrightarrow \phi(r) &= \frac{1}{2\sqrt{2\pi}} \frac{e}{4\pi\epsilon_0} \sum_n A_n n! \lim_{b \rightarrow 0} \left[- \int_{-\infty}^{\infty} e^{i\frac{\pi}{2}\omega} \frac{u(-\omega) e^{b\omega} e^{i\omega r} d\omega}{(a_n + i\omega)^{n+1}} + \int_{-\infty}^{\infty} e^{i\frac{\pi}{2}\omega} \frac{u(\omega) e^{-b\omega} e^{i\omega r} d\omega}{(a_n + i\omega)^{n+1}} \right] \end{aligned}$$

The definition of the sign-function was utilized here. Also note that the imaginary value can be mapped to the real axis by phase rotation.

$$sgn(\omega) = \lim_{b \rightarrow 0} u(-\omega) e^{b\omega} + \lim_{b \rightarrow 0} u(\omega) e^{-b\omega} \text{ and } u(\omega) = \begin{cases} 1 & \omega > 0 \\ 0 & \omega < 0 \end{cases}$$

By integration the following expression is obtained.

$$\Leftrightarrow \phi(r) = \frac{e}{4\pi\epsilon_0} \sum_n \left(-\frac{1}{2} \frac{A_n}{2\sqrt{2\pi}} \lim_{b \rightarrow 0} [\theta(r+b)(r+b)^n e^{-a_n(-r-b)}]_{-\infty}^{\infty} \right. \\ \left. + \frac{1}{2} \frac{A_n}{2\sqrt{2\pi}} \lim_{b \rightarrow 0} [\theta(r-b)(r-b)^n e^{-a_n(r-b)}]_{-\infty}^{\infty} \right)$$

Now one swaps the integration limits on the left and substitutes with $-r$

$$\Leftrightarrow \phi(r) = \frac{e}{4\pi\epsilon_0} \sum_n \left(\frac{1}{2} \frac{A_n}{2\sqrt{2\pi}} \left\{ \lim_{b \rightarrow 0} [\theta(r-b)(r-b)^n e^{-a_n(r-b)}]_{-\infty}^{\infty} \right. \right. \\ \left. \left. + \lim_{b \rightarrow 0} [\theta(r-b)(r-b)^n e^{-a_n(r-b)}]_{-\infty}^{\infty} \right\} \right) \\ \Leftrightarrow \phi(r) = \frac{1}{\sqrt{2\pi}^3} \frac{e}{4\pi\epsilon_0} \sum_n \int_{-\infty}^{\infty} \frac{A_n n!}{(a_n + i\omega)^{n+1}} \operatorname{sgn}(\omega) e^{i\frac{\pi}{2}} e^{i\omega r} d\omega \\ = \frac{1}{2\sqrt{2\pi}} \frac{e}{4\pi\epsilon_0} \sum_n A_n r^n e^{-a_n r} \quad (9)$$

It is important to note that the Schrodinger equation does not refer to the potential ϕ , but the potential energy V , i.e., this is obtained by multiplying ϕ by e :

$$V(r) = e\phi(r) = \frac{1}{2\sqrt{2\pi}} \frac{e^2}{4\pi\epsilon_0} \sum_n A_n r^n e^{-a_n r} \quad (10)$$

Thus (10) results in a formulation of a radial symmetric electron potential energy, which can be processed and integrated in the Schrodinger equation. $V(r)$ describes the situation, that every potential caused by electrons present in the vicinity of the atom can be modelled as a sum over n of a polynomial expression multiplied with an exponential damped probability depending on the distance to the core with the specific parameters A_n and a_n . This formulation will be used in the following chapters. In the case of helium in the ground state, a coupling constant f_E is also required to consider the effects of vacuum polarization. May f_E be introduced here formally, then the specific formula of $V^e(r)$ used here is therefore as follows:

$$V^e(r) = \frac{f_E}{2\sqrt{2\pi}} \frac{e^2}{4\pi\epsilon_0} \sum_n A_n r^n e^{-a_n r} \quad (11)$$

The motivation and derivation of f_E is presented in the following chapter.

5. Corrections of the electromagnetic coupling of the electrons by vacuum polarization

A closer reflection of the electron state configuration in Chapter 3 raises the question of how the electrons are actually distributed in the wave function. Without multipole moment and without orbital angular momentum or spin, both wave functions are de facto congruent. Not only are the electrons interchangeable and thus indistinguishable, but they also occupy virtually the same space at the same time, i.e. they may come very close to each other, namely much closer than to the nucleus, for example. Under these conditions, Coulomb's law is only approximately valid, and the interaction mechanisms from quantum electrodynamics must also be considered [21-41]. This can be visualized as follows: Vacuum polarization, i.e., the reversible temporary virtual decay of a photon into an electron-positron pair, shields parts of the electromagnetic field of a real charge, so that the limit case of Coulomb's law is fulfilled for large distances. At much smaller distances, this shielding effect is significantly reduced, and additional terms must be considered for physical correctness. The charge appears stronger from the immediate vicinity, that means the coupling constant between two charges must be adjusted. Only low-order approximations are used in this report, and these are known in the literature as the Wichmann-Kroll potential and the Uehling potential [24,31,34,35].

First consider the Uehling potential, defined in the literature [34] as the integral:

$$V_U(r) = -Z\alpha\hbar c \frac{1}{r} \left(1 + \frac{2\alpha}{3\pi} \int_1^\infty e^{-4\pi rx/\lambda} \frac{2x^2 + 1}{2x^4} \sqrt{x^2 - 1} dx \right)$$

λ corresponds to the Compton wavelength of the electron and α is Sommerfeld's fine structure constant. The integral cannot be represented with elementary functions, but this is not necessary for our case. If the equation is approximated for small distances $\frac{\lambda}{r} \gg 2\pi \exp\left(\gamma + \frac{5}{6}\right)$, where γ is the Euler-Mascheroni constant, the following results:

$$V_U(r)|_{r \rightarrow 0} = -Z\alpha\hbar c \frac{1}{r} \left(1 + \frac{2\alpha}{3\pi} \left(\ln\left(\frac{\lambda}{2\pi r}\right) - \gamma - \frac{5}{6} \right) \right) + \mathcal{O}(\alpha^3) \quad (12)$$

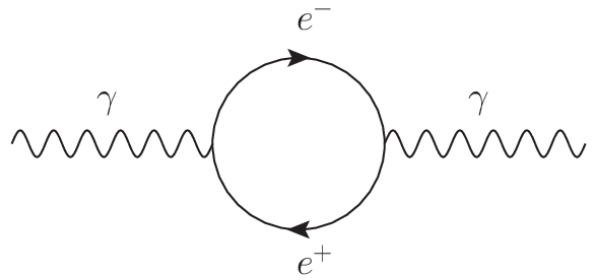


Fig.1: Feynmann diagram of the lowest-order vacuum polarization: A photon decays into a virtual electron-positron pair, which shortly afterwards decays again to a photon. Electrons and positrons cannot be detected as they are virtual, but their effect can be very well, as this allows an existing electric field of a real particle to be partially shielded [21].

The Uehling potential plays an important role especially in the vicinity of heavy nuclei, but in our case, it is only of secondary importance in the interaction of two low-energy bound electrons, as can easily be determined mathematically by considering the Compton wavelength for electrons $\lambda_e = 2.426 * 10^{-12} m$.

Much more important is the influence of the Wichmann-Kroll potential, which is defined in the literature as [31]:

$$W_K(r) = \frac{2\hbar Q^3 e^7}{225\pi m_e^4 c^7 (4\pi)^4 r^5} \quad (13)$$

One can see the difference to Coulomb's law, because here the influence of the field decreases with the 5th power, i.e., for large distances only the classic Coulomb potential will remain effective. At small distances between the two charges, however, $W_K(r)$ will lead to significant deviations and must be considered as an additional coupling.

If we now follow the idea of two electrons approaching each other, which have no way of avoiding due to the constraint of the orbital bond, then the approach of pure point-like particles is no longer expedient. However, electrons do not exhibit an internal structure, as far as is known from current research and literature [29, 30, 36, 37, 38], which is why the most general approach possible should be used without any prior assumptions. A distribution in the form of a Gaussian function with an imaginary electron radius r_e is therefore used.

$$\psi_e(r) = f_e e^{-\frac{1}{2}(\frac{r}{r_e})^2} \text{ mit } f_e^2 \int_0^{\infty} |\psi_e(r)|^2 dr = 1 \Leftrightarrow f_e^2 = \frac{2}{\sqrt{\pi} r_e} \quad (14)$$

The radius is not to be understood as a fixed surface, but in accordance with the principles of quantum mechanics, the area with the highest probability density. However, it is important to note that this is not the wave function of the electron in the helium atom - this will be considered in the next chapter. Here the distance related effects of both particle wave functions shall be modeled.

The particles are evaluated as a function of their distance, which is why we remain in one-dimensional space - in contrast to the Schrödinger equation, which is evaluated in three dimensions. Basically, not the distance between two manifested particles is considered here like two marbles facing each other, but the virtual distance between two orbitals lying exactly on top of each other, whose particle wave functions have a non-zero amplitude simultaneously at each location in the vicinity of the atom.

If one now evaluates the Wichmann-Kroll potential with the above distribution using the given method of the convolution product via Fourier transformation, we obtain the following result.

First, consider the Fourier transform of the potential from (13):

$$\mathcal{F}(W_K(r))(\omega) = \mathcal{F}\left(\frac{2\hbar Q^3 e^7}{225\pi m_e^4 c^7 (4\pi)^4 r^5}\right)(\omega) = \frac{2\hbar Q^3 e^7}{225\pi m_e^4 c^7 (4\pi)^4} \frac{i}{24} \sqrt{\frac{\pi}{2}} \omega^4 \operatorname{sgn}(\omega)$$

The Fourier Transform of the electron wave function results in:

$$\mathcal{F}(\rho(r))(\omega) = \mathcal{F}(f_e^2 |\psi_e(r)|^2)(\omega) = f_e^2 \frac{r_e}{\sqrt{2}} e^{-\frac{1}{4}r_e^2 \omega^2} = \sqrt{\frac{2}{\pi}} e^{-\frac{1}{4}r_e^2 \omega^2}$$

One obtains the product for the inverse Fourier Transform to:

$$\begin{aligned} W_K^e(r) &= \mathcal{F}^{-1}\left(\frac{2\hbar Q^3 e^7}{225\pi m_e^4 c^7 (4\pi)^4} \frac{1}{24} \sqrt{\frac{\pi}{2}} \omega^4 \operatorname{sgn}(\omega) e^{i\frac{\pi}{2}} \sqrt{\frac{2}{\pi}} e^{-\frac{1}{4}r_e^2 \omega^2}\right) \\ &\Leftrightarrow W_K^e(r) = \frac{\sqrt{2}\hbar e^{10}}{675\pi m_e^4 c^7 (4\pi)^4} e^{-\left(\frac{r}{r_e}\right)^2} \frac{3r_e^4 - 12r_e^2 r^2 + 4r^4}{r_e^9} \end{aligned} \quad (15)$$

Thus (15) describes the Wichmann-Kroll potential for an electron in the form of an extended charge distribution. The question now arises as to what happens when two electrons come closer and closer together. If we consider the energy of one electron in the potential (15) of a second:

$$\Leftrightarrow E_{W_K^e} = \langle \psi_e(r - r') | W_K^e(r) | \psi_e(r - r') \rangle \text{ minimal}$$

If there is a stable point for both electrons, this must manifest in a minimum potential energy. If r' is the distance of the second electron, then the situation can be expressed as follows:

$$\begin{aligned} &\Leftrightarrow \frac{\partial}{\partial r'} \int_0^\infty \frac{\sqrt{2}\hbar e^{10}}{675\pi m_e^4 c^7 (4\pi)^4} e^{-\left(\frac{r}{r_e}\right)^2} \frac{3r_e^4 - 12r_e^2 r^2 + 4r^4}{r_e^9} \sqrt{\frac{2}{\pi}} e^{-\left(\frac{r-r'}{r_e}\right)^2} dr = 0 \\ &\Leftrightarrow -\frac{2\sqrt{2}\hbar e^{10}}{675\pi \sqrt{\pi} m_e^4 c^7 (4\pi)^4} \frac{\partial}{\partial r'} \left(\frac{2r_e(7r'e^2 - r'^3) + \sqrt{2\pi}(3r_e^4 - 6r'^2 r_e^2 + r'^4) e^{\frac{1}{2}(\frac{r'}{r_e})^2} \operatorname{erf}\left(-\frac{r'}{\sqrt{2}r_e}\right) e^{-\left(\frac{r'}{r_e}\right)^2}}{16r_e^8} \right) = 0 \\ &\Leftrightarrow -\frac{2\sqrt{2}\hbar e^{10}}{675\pi \sqrt{\pi} m_e^4 c^7 (4\pi)^4} \left(\frac{2r_e(4r_e^4 - 11r'^2 r_e^2 + r'^4) + \sqrt{2\pi}r'(15r_e^4 - 10r'^2 r_e^2 + r'^4) \operatorname{erf}\left(\frac{r'}{\sqrt{2}r_e}\right) e^{\frac{1}{2}(\frac{r'}{r_e})^2} e^{-\left(\frac{r'}{r_e}\right)^2}}{16r_e^{10}} \right) = 0 \end{aligned}$$

For simplification, substitute with $r' = ar_e$, $a > 0$, then the extremes can be evaluated by analyzing the first and second derivatives:

$$\frac{\partial E_{W_K^e}}{\partial a}(a) = -\frac{2\sqrt{2}\hbar Q^3 e^7}{675\pi \sqrt{\pi} m_e^4 c^7 (4\pi)^4} \left(\frac{8 - 22a^2 + 2a^4 + \sqrt{2\pi}ae^{\frac{1}{2}a^2}(15 - 10a^2 + a^4)\operatorname{erf}\left(\frac{a}{\sqrt{2}}\right)}{16r_e^5} e^{-a^2} \right) = 0$$

$$\frac{\partial^2 E_{WK}^e}{\partial a^2}(a) = -\frac{2\sqrt{2}\hbar Q^3 e^7}{675\pi\sqrt{\pi}m_e^4 c^7 (4\pi)^4} \left(\frac{-2a(15 - 16a^2 + a^4) - \sqrt{2\pi}e^{\frac{1}{2}a^2}(-15 + 45a^2 - 15a^4 + a^6)erf\left(\frac{a}{\sqrt{2}}\right)}{16r_e^5} e^{-a^2} \right)$$

This results in the following roots via numerical calculation: $\frac{\partial E_{WK}^e}{\partial a}(a) = 0$

$$r_1 = 1.10628r_e, \quad \frac{\partial^2 E_{WK}^e}{\partial a^2}\left(\frac{r_1}{r_e}\right) > 0 \Leftrightarrow \text{local minimum}$$

$$r_2 = 2.85945r_e, \quad \frac{\partial^2 E_{WK}^e}{\partial a^2}\left(\frac{r_2}{r_e}\right) < 0 \Leftrightarrow \text{local maximum}$$

The relevant zero point is $r_{min} = 1.106r_e = a_{min}r_e$. Therefore, surprisingly an energetically stable point of both electrons can be found at a distance of $a_{min}r_e$ and an energy of $E_{WK}^e(a_{min}r_e) = -8.01 \text{ neV}$. The situation can also be interpreted in such a way that both electrons are coupled at this point and in the absence of stronger fields or corresponding collision processes that would break this connection again - behave like an independent particle with zero spin and zero angular momentum. This effect can also be seen in Figure 2, where the pronounced minimum at $r = a_{min}r_e$ is clearly visible. The low energy threshold of - 8.01 neV makes it obvious that the entangled connection between the two electrons with spin 0 – characterized by specific bosonic behavior - is quite delicate and can easily be disturbed. If one considers the threshold in relation to the thermal energy, then possible entanglement phenomena with features that are found for bosons - this could be superfluidity, for example - with $E_{WK}^e > kT$ - will become significantly measurable below approx. 0.1 mK. This is in fact described in the literature [42-47], though the λ -point, i.e., the pressure dependent temperature where helium becomes superfluid, is described to be at 2.17K @ 5036Pa for ${}^4\text{He}$. For a further investigation of the phenomena with this mathematical approach, however, additional statistical tools, such as the Bose-Einstein statistics for S=0 respectively, are to be used. In addition, only lower-order approximations from quantum electrodynamics are considered here; a more precise analysis

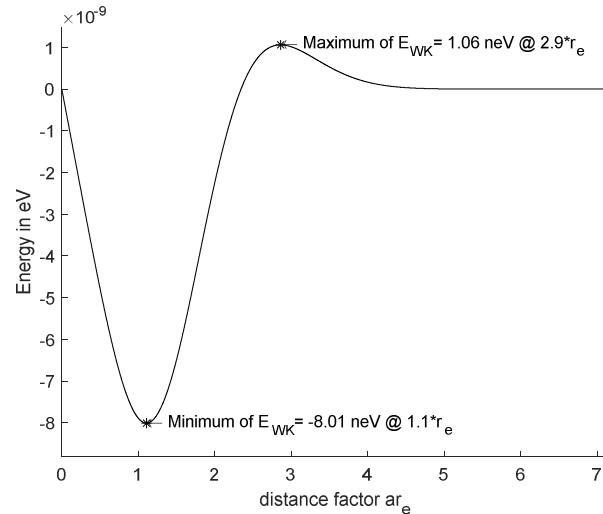


Fig.2: Behavior of the energy E_{WK}^e in relation to the distance function $r = ar_e$. You can clearly see the minimum formed at $1.1 r_e$ and somewhat weaker the maximum at $2.9 r_e$. It is easy to guess that at a relative energy threshold of - 35.8 neV, even small disturbances are sufficient to break the entanglement. Nevertheless, both electrons in the compound generate a significant increase in the coupling factor for V^e

probably also requires the consideration of higher perturbation terms. And last but not least, a comparison with experimental data should be considered, whereby a preparation with pure $1s^2$ 1S_0 helium would be important here, because ortho helium will behave differently due to its different spin configuration. This is a task for future investigations.

Regardless of the temperature, the minimum of E_{WK}^e refers to the mean distance between the two electrons. The actual constraint for the bond or the position of the electrons is of course still the Coulomb potential of the nucleus, without both electrons would immediately move apart thus breaking this bond. The actual relevant wave function for the electrons can be found in Chapter 6.

To determine a correction factor, we now consider the total potential of the electron with the modified Wichmann-Kroll potential for the electron:

$$V^e = V_C^e + W_K^e = \left(\frac{e^2}{4\pi\epsilon_0 r} - \frac{\sqrt{2}\hbar e^{10}}{675\pi m_e^4 c^7 (4\pi)^4} e^{-\left(\frac{r}{r_e}\right)^2} \frac{3r_e^4 - 12r_e^2 r^2 + 4r^4}{r_e^9} \right)$$

V^e must be repulsive due to the electron-electron interaction. The proximity of the electrons reduces the shielding effect of vacuum polarization. Contraction of the equation leads to:

$$\Leftrightarrow V^e = \frac{e^2}{4\pi\epsilon_0 r} \left(1 - r \frac{4\pi\epsilon_0 \sqrt{2}\hbar e^8}{675\pi m_e^4 c^7 (4\pi)^4} e^{-\left(\frac{r}{r_e}\right)^2} \frac{3r_e^4 - 12r_e^2 r^2 + 4r^4}{r_e^9} \right) \quad (16)$$

If one inserts now $r_{min} = 1.106r_e = a_{min}r_e$ as the stable distance, this results in:

$$\begin{aligned} \Leftrightarrow V^e|_{r_{min}} &= \frac{e^2}{4\pi\epsilon_0 r} \left(1 - a_{min} \frac{4\sqrt{2}\epsilon_0 \hbar e^8}{675m_e^4 c^7 (4\pi)^4} e^{-a_{min}^2} \frac{3 - 12a_{min}^2 + 4a_{min}^4}{r_e^4} \right) \\ \Leftrightarrow V^e|_{r_{min}} &= \frac{e^2}{4\pi\epsilon_0} \left(1 - \frac{K_{E_min}}{r_e^4} \right) \frac{1}{r} \end{aligned} \quad (17)$$

With the simplification by K_{E_min}

$$K_{E_min} = \frac{4\sqrt{2}\epsilon_0 \hbar e^8}{675m_e^4 c^7 (4\pi)^4} e^{-a^2} a_{min} (3 - 12a_{min}^2 + 4a_{min}^4)$$

By anticipating the solution from Chapter 6 to a certain extent, the coupling factor can be calculated from the Schrodinger equation using the energy values for the helium ground state that are sufficiently known from the literature [73-77]:

$$\begin{aligned} \frac{e^2}{4\pi\epsilon_0} \left(1 - \frac{K_{E_min}}{r_e^4} \right) &\equiv f_E \frac{e^2}{4\pi\epsilon_0} \Leftrightarrow f_E = 1 - \frac{K_{E_min}}{r_e^4} \\ \Leftrightarrow \sqrt[4]{\frac{K_{E_min}}{1 - f_E}} &= r_e = 3.4062 * 10^{-36} m \end{aligned} \quad (18)$$

Here, $f_E \cong 12.312$ is the numerically determined coupling constant to reproduce $E_0 = -24.6\text{eV}$. This gives the half-width of the electron radius r_e . Since a Gaussian distribution was applied, the 3σ diameter of the electron is thus $2.044 * 10^{-35}\text{m}$ and corresponds very well with the Planck length of $l_P = 1.62 * 10^{-35}\text{m}$. The electron can therefore actually be regarded as a point-like particle in the context of this observation, and it can enter entanglements via the connection of the Wichmann-Kroll potential, though pure bosonic states can only be found in the mK-range because of the low binding energy. To recall shortly the former discussion, the location of the particle is not considered here. In principle, it is difficult to describe the surface of particles at these length scales using quantum mechanics; only zones of localization density can be meaningfully defined. The electron probability density is described by the wave functions and these constraints both electrons simultaneously. Here the question is discussed how two electrons can occupy the same place at the same time and what effects can be expected if both are in superposition down to a virtual distance of 0. The derivation in this chapter suggests that both electrons in the helium atom are in a quasi-entangled state and behave like a particle with spin 0. True entanglement starts to be noticeable in the mK-range. The mean distance for the local energy minimum of both electrons can be derived as:

$$r_{min} = a_{min}r_e = 1.106 * r_e = 3.767 * 10^{-36}\text{m}$$

If we now consider a virtual distance-perturbation at the point $r_{min} = 1.106r_e = a_{min}r_e$ in order to find out how the system reacts to fluctuations between the electrons, one finds:

$$\frac{\partial}{\partial r} V^e \Big|_{r_{min}} = -\frac{e^2}{4\pi\epsilon_0} \left(1 - \frac{K_{E_min}}{r_e^4}\right) \frac{1}{(a_{min}r_e)^2} \approx -2,00 * 10^{44} \frac{J}{m} \approx -32.05 \frac{GeV}{fm} \quad (19)$$

This means that if an electron is slightly removed from the helium nucleus, or if both electrons move apart from each other by collisions or through excitation, the system reacts with a very high

amplitude by lowering the potential energy and thus by lowering the coupling factor very significantly. hence, the small repulsive coupling factor increases the binding potential component of the nucleus i.e., the total potential of the helium system counteracts a distance disturbance of the electrons much more strongly than in the hydrogen atom. If, on the other hand, the electron is pushed towards the nucleus, the energy of the system increases accordingly and in turn counteracts the movement.

Obviously, this correlation provides a plausible explanation to the chemical stability of helium and why systems with closed shells in general are stable against external disturbances below the binding energy and hence chemical reactions. Thus, a fundamental mechanism of the inertia of closed-shell systems towards chemical reactions, as it is typical for noble gases can be shown here.

To complete the discussion in this chapter it is also worth mentioning that the influence of the coupling factor f_E also prohibits the orthogonality of the wave functions with different n as one is used to the well-known analytical solutions of the Hydrogen atom. For excited states, i.e., states where the two electrons have a significant distance like $(1s, 2s)$ or $(1s, 2p)$, the exchange interaction and thus the coupling factors are significantly small. So, these states can very well be approximated by superpositions of the Hydrogen solution. But the closer the two electrons get the more they interact with the declining influence of vacuum polarization, and the result is a significantly disturbed wave function to the point where the original Hydrogen solution does not represent the real physical situation anymore.

6. The analytical solution of the Schrodinger equation for Helium

Finally, we need to solve the Schrodinger equation. The derived electron potential together with the radially symmetric wave function results in $R(r)$. Note that both the Coulomb and the exchange term must be taken into account for the electron potential [14].

$$\frac{\partial^2 R}{\partial r^2} + \frac{2}{r} \frac{\partial R}{\partial r} + \frac{2m_e}{\hbar^2} \left(\frac{Ze^2}{4\pi\epsilon_0} \frac{1}{r} - \frac{\hbar^2 l(l+1)}{2m_e r^2} - f_E \frac{e^2}{4\pi\epsilon_0} \left(\frac{1}{r} \right) * (V_C + V_A) + E \right) R = 0 \quad (20)$$

(20) is a particularly challenging task due to the non-linear potential term of the electrons. Therefore, only the ground state for the two-electron atom with $l = 0$ is considered here in a simplified way and the following substitution is inserted simultaneously:

$$A \equiv \frac{2m_e}{\hbar^2} \frac{Ze^2}{4\pi\epsilon_0}, \quad B \equiv \frac{2m_e}{\hbar^2}, \quad C_E \equiv \frac{2m_e}{\hbar^2} \frac{f_E}{2\sqrt{2\pi}} \frac{e^2}{4\pi\epsilon_0} \quad (21)$$

One ought to note that the term $\frac{f_E}{2\sqrt{2\pi}} \frac{e^2}{4\pi\epsilon_0}$ for C_E is derived in the previous chapters with the correct coupling. Accordingly, a coupled differential equation must also be used for helium as a two-electron system:

$$1.) \frac{\partial^2 R_1}{\partial r^2} + \frac{2}{r} \frac{\partial R_1}{\partial r} + \left(\frac{A}{r} + BE \right) R_1 - C_E r^2 R_2 R_2 R_1 - C_E r^2 R_1 R_2 R_1 = 0$$

$$2.) \frac{\partial^2 R_2}{\partial r^2} + \frac{2}{r} \frac{\partial R_2}{\partial r} + \left(\frac{A}{r} + BE \right) R_2 - C_E r^2 R_1 R_1 R_2 - C_E r^2 R_1 R_2 R_2 = 0$$

The Coulomb interaction is represented here by $C_E r^2 R_j R_j R_i$ and the exchange interaction by $C_E r^2 R_j R_i R_i$, where $i \neq j$ applies.

For further work, it has proven to be useful to transform the differential equation into Laplace space [55-64]. The Laplace transformation requires functions defined on \mathbb{R}_0^+ and integrable functions with lower growth than e^{st} with $t \rightarrow +\infty$. This is the case for the wave functions sought here. However, reciprocal r-terms cause difficulties during the transformation, which is why they are multiplied by $r \neq 0$ beforehand:

$$\Leftrightarrow r \frac{\partial^2 R_i}{\partial r^2} + 2 \frac{\partial R_i}{\partial r} + (A + rBE) R_i - C_E r^2 |R_j|^2 r R_i - C_E r^2 |R_i|^2 r R_j = 0 \quad (22)$$

Now translate (22) into the Laplace transform according to the conversion rules from [61,62,63]. Let $\mathfrak{R}_i(s) = \mathcal{L}_r[R_i(r)](s)$ be the Laplace transform of the wave function. In addition,

$$\mathcal{L}_r[r^2 |R_i|^2](s) \equiv \mathfrak{f}_i$$

should be defined to facilitate processing later. This results in the Laplace-transformed Schrodinger equation as:

$$\begin{aligned} -s^2 \frac{\partial}{\partial s} \mathfrak{R}_i(s) - 2s \mathfrak{R}_i(s) + R_i(0) + 2(s \mathfrak{R}_i(s) - R_i(0)) + A \mathfrak{R}_i(s) - BE \frac{\partial}{\partial s} \mathfrak{R}_i(s) + C_E \mathfrak{f}_j \\ * \frac{\partial}{\partial s} \mathfrak{R}_i(s) + C_E \mathfrak{f}_i * \frac{\partial}{\partial s} \mathfrak{R}_j(s) = 0 \end{aligned}$$

First one ought to simplify the equations:

$$\Leftrightarrow -(s^2 + BE) \frac{\partial}{\partial s} \mathfrak{R}_i(s) + A \mathfrak{R}_i(s) - R_i(0) + C_E \mathfrak{f}_j * \frac{\partial}{\partial s} \mathfrak{R}_i(s) + C_E \mathfrak{f}_i * \frac{\partial}{\partial s} \mathfrak{R}_j(s) = 0 \quad (23)$$

Before continuing, two important theorems from functional analysis should be mentioned. The first is the theorem of Fubini and Tonelli, which states that the integral of a convolution of two non-negative functions is equal to the multiplication of the two function integrals [48,49]. The respective functions must be doubly integrable. For our case, this means:

$$\int_0^\infty [\mathfrak{F}(s) * \mathfrak{G}(s)] ds = \int_0^\infty \mathfrak{F}(s) ds \int_0^\infty \mathfrak{G}(s) ds \quad (24)$$

The second important theorem is the Parseval-Plancherel identity, which states that the integral of the squared functions is identical in both spatial and - in this case - Laplace space [51-54]. The Parseval-Plancherel identity also applies to other transformations, but is of importance here for the Laplace transformation:

$$\int_0^\infty |F(r)|^2 dr = \int_0^\infty |\mathfrak{F}(s)|^2 ds \quad (25)$$

As the identity $\frac{\partial}{\partial s} \int ds = \mathbb{I}$ is now applied to (23) and (25) is used to take into account that $\int_0^\infty \mathfrak{f}_i ds = \int_0^\infty r^2 |R_i|^2 dr = 1$, then the equation results in particular from (24):

$$\frac{\partial}{\partial s} \int_0^\infty \left[\mathfrak{f}_i * \frac{\partial}{\partial s} \mathfrak{R}_j \right] ds = \frac{\partial}{\partial s} \int_0^\infty \mathfrak{f}_i ds \int_0^\infty \frac{\partial}{\partial s} \mathfrak{R}_j ds = \frac{\partial}{\partial s} \int_0^\infty \frac{\partial}{\partial s} \mathfrak{R}_j ds = \frac{\partial}{\partial s} \mathfrak{R}_j$$

So, this results in:

$$-(s^2 + BE - C_E) \frac{\partial}{\partial s} \mathfrak{R}_i(s) + A \mathfrak{R}_i(s) - R_i(0) + C_E \frac{\partial}{\partial s} \mathfrak{R}_j(s) = 0$$

If one now uses the derived identity $\mathfrak{R}_1(s) \equiv \mathfrak{R}_2(s) \equiv \mathfrak{R}(s)$ from chapter 3, the system of two differential equations can be merged by inserting them and obtaining the result by rearranging the equation:

$$\frac{\partial}{\partial s} \mathfrak{R}(s) = -\frac{s^2 + BE}{(s^2 + BE - C_E)^2 - C_E^2} A \mathfrak{R}(s) + \frac{s^2 + BE}{(s^2 + BE - C_E)^2 - C_E^2} R(0) \quad (26)$$

By the way – it is obvious from (26), that $\frac{\partial}{\partial s} \mathfrak{R}(s)$ is nonnegative over \mathbb{R}_0^+ as well as \mathfrak{f}_i , so (24) is applicable here. The inverse Transform to the spatial r -dimension is once again straight forward [see 63]:

$$R(r) = \frac{A}{r} \left(\frac{\sinh(r\sqrt{2C_E - BE})}{2\sqrt{2C_E - BE}} \right) * R(r) + R(0) \frac{A}{r} \left(\frac{\sinh(r\sqrt{2C_E - BE})}{2\sqrt{2C_E - BE}} \right) \quad (27)$$

Before continuing, the equation is simplified with the substitution $\alpha^2 = 2C_E - BE$. Since the binding energy is conventionally less than zero, the root remains real. Again, analogous to (24), the theorem of Fubini and Tonelli can be used, and the result is obtained by applying the identity $\frac{\partial}{\partial r} \int dr = \mathbb{I}$, this time in local r -space:

$$\begin{aligned} \frac{\partial}{\partial r} \int_0^\infty R(r) dr &= \frac{\partial}{\partial r} \left[\int_0^\infty \frac{A}{r} \left(\frac{\sinh(ar)}{2\alpha} \right) dr \int_0^\infty R(r) dr + R(0) \int_0^\infty \frac{A}{r} \left(\frac{\sinh(ar)}{2\alpha} \right) dr \right] \\ &\Leftrightarrow \frac{\partial}{\partial r} \left[\int_0^\infty R(r) dr \left(1 - \int_0^\infty \frac{A}{r} \left(\frac{\sinh(ar)}{2\alpha} \right) dr \right) \right] = \frac{\partial}{\partial r} \left[R(0) \int_0^\infty \frac{A}{r} \left(\frac{\sinh(ar)}{2\alpha} \right) dr \right] \\ &\Leftrightarrow R(r) = \frac{\partial}{\partial r} \int_0^\infty R(r) dr = \frac{\partial}{\partial r} \left[\frac{R(0) \int_0^\infty \frac{A}{r} \left(\frac{\sinh(ar)}{2\alpha} \right) dr}{1 - \int_0^\infty \frac{A}{r} \left(\frac{\sinh(ar)}{2\alpha} \right) dr} \right] \\ &\Leftrightarrow R(r) = R(0) \frac{\alpha^3}{2A} \frac{rsinh(ar)}{\left(\frac{\alpha^2}{A} r + cosh(ar) \right)^2} \end{aligned} \quad (28)$$

$R(r)$ is the analytically derived radial part of the wave function for helium in the ground state – as well as helium-like systems with $n=1$, $S=0$, $L=0$. Since $R(r)$ is well-defined, $R(0)$ is regarded as $\lim_{a \rightarrow 0} R(a)$, $a > 0$. The wave function is normalized over f_N and is obtained:

$$R(r) = f_N \frac{rsinh(ar)}{\left(\frac{\alpha^2}{A} r + cosh(ar) \right)^2} = 2f_N \frac{r(e^{ar} - e^{-ar})}{\left(\frac{2\alpha^2}{A} r + e^{ar} + e^{-ar} \right)^2} \quad (29)$$

Therefore, normalization for the wave function is still valid by the equation:

$$\int_0^\infty r^2 |R|^2 dr \equiv \frac{1}{f_N^2}, \quad f_N > 0$$

One finds documented in the annex, that (29) is covered by the formula of the general electron potential proven in chapter 4 and hence that the shown approach is valid. It should also be mentioned that there is no analytical root function for the integral to determine f_N . The integral is consequently integrated numerically. Resubstitute for α and A then one finds:

$$\alpha^2 = 2C_E - BE = \frac{2m_e}{\hbar^2} \left(\frac{f_E}{\sqrt{2\pi}} \frac{e^2}{4\pi\epsilon_0} + |E_0| \right), \quad A \equiv \frac{2m_e}{\hbar^2} \frac{Ze^2}{4\pi\epsilon_0} \quad (30)$$

If we look at the behavior at $r \rightarrow 0$ and $r \rightarrow \infty$, we see that $R(r)$ disappears for both points: $\lim_{r \rightarrow 0} R(r) \rightarrow 0$ and $\lim_{r \rightarrow \infty} R(r) \rightarrow 2f_N e^{-\alpha r}$. A direct comparison with the original hydrogen solution of the Schrodinger equation reveals interesting differences. So, if we look at the radial probability density for both cases, one notifies:

$$r^2 |R_{1,0,0}^H(r)|^2 = \frac{2}{\pi a_0^3} r^2 e^{-\frac{4r}{a_0}} \quad \text{and} \quad r^2 |R_{1,0,0}^{He}(r)|^2 = f_N^{-2} \frac{r^4 \sinh^2(\alpha r)}{\left(\frac{\alpha^2}{A} r + \cosh(\alpha r) \right)^4}$$

With the known Bohr radius $a_0 = \frac{4\pi\epsilon_0\hbar^2 n^2}{Ze^2 m_e}$ and the decay constant α for the helium solution. If a_0^{-1} and α were to be understood as concrete radii, then it is noticeable that helium with the wave function derived in this report would be smaller than the radius of the hydrogen atom by a factor of about 0.74 at 39.6 pm, which would be in very good agreement with the literature [64-72]:

$$\begin{aligned} \text{Helium:} \quad \alpha &= \sqrt{\frac{2m_e}{\hbar^2} \left(\frac{f_E}{\sqrt{2\pi}} \frac{e^2}{4\pi\epsilon_0} + |E_0| \right)} \\ \text{Hydrogen:} \quad \frac{1}{a_0} &= \frac{2m_e}{\hbar^2} \frac{1}{2} \frac{e^2}{4\pi\epsilon_0} = \sqrt{\frac{2m_e |E_0|}{\hbar^2}} \end{aligned} \quad (31)$$

However, this is misleading because α has a different meaning as a decay constant of the wave function than a_0^{-1} . This becomes clear from the comparison - the literature shows Bohr's radius of 52.9 pm as the maximum probability density for hydrogen. In contrast, helium shows a maximum probability density at 96.7 pm, i.e., almost twice the amount, as can be seen in Fig. 4. However, due to the 1.34 times higher damping constant for helium, the probability density of the electron decreases much faster than for hydrogen. At the same time, it is noticeable for $r \rightarrow 0$ that $R_{1,0,0}^{He}$ in helium behaves like $r \sinh(\alpha r) \approx 2\alpha r^2$, i.e. the radial probability density per shell element dr almost completely disappears in proportion to r^6 in the vicinity of the core. This is also understandable, as the presence of the two electrons would cause the energy density at the nucleus to diverge due to the mutual repulsion of the two electrons in this very small spatial element. Consequently, the probability of the electrons being present shifts outwards - away from the nucleus. So, the closed

1S-electron shell is obviously much more compact and denser than the non-closed shell of hydrogen due to the influence of the quantum electrodynamic interaction of the two electrons. This makes it plausible that although the highest electron density appears somewhat further away from the nucleus, the helium atom appears smaller from the outside due to the higher decay constant of the wave function. This leads to the intriguing fact that the helium atom appears to be comparable in size to the hydrogen atom, while the electrons are located denser around the core.

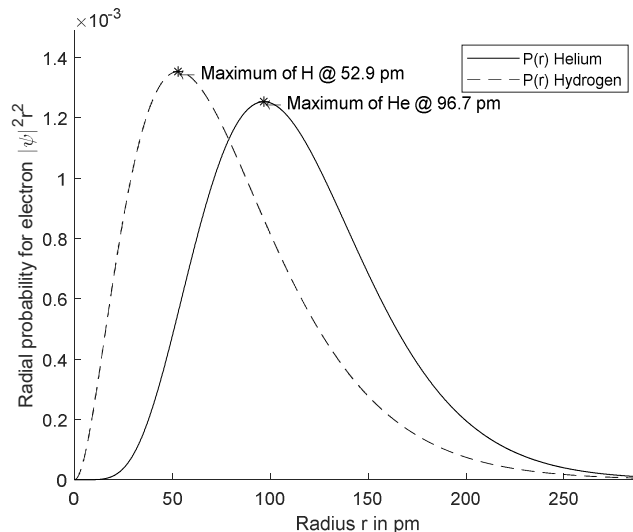


Fig.4: Radial probability density for the helium atom (red) and the hydrogen atom (green). It is noticeable that the maximum of the distribution is at 52.9 pm, as known from the literature, while the electrons in helium have their maximum probability density at 96.7 pm. In contrast, helium shows a much steeper drop in the distribution.

7. Energy determination of the neutral Helium in the ground state

Now one important step is still missing, namely the energy determination from the Schrodinger equation according to the calculation rule:

$$\langle r^2 R(r) Y_{0,0}(\varphi, \psi) | \hat{H} | r^2 R(r) Y_{0,0}(\varphi, \psi) \rangle = E \quad (32)$$

Since only the ground state has been considered here so far, (24) is reduced to the radial part. This results in the following formulation:

$$\begin{aligned} & \Leftrightarrow \int_0^\infty r^2 R^* \frac{d^2 R}{dr^2} dr + \int_0^\infty r^2 R^* \frac{2}{r} \frac{dR}{dr} dr + \int_0^\infty r^2 \left(\frac{A}{r} + BE \right) |R|^2 dr - 2C_E \int_0^\infty r^4 (|R|^2)^2 dr = 0 \\ & \Leftrightarrow \frac{1}{B} \int_0^\infty r^2 R^* \frac{d^2 R}{dr^2} dr + \frac{2}{B} \int_0^\infty r R^* \frac{dR}{dr} dr + \frac{A}{B} \int_0^\infty r |R|^2 dr - \frac{2C_E}{B} \int_0^\infty r^4 (|R|^2)^2 dr = -E \end{aligned}$$

Now it is important to mention that $R(r)$ already contains the energy in the decay constant α according to (31) and (32). It is therefore a recursive formula that cannot be solved explicitly. However, $\frac{dR}{dr}$ and $\frac{d^2 R}{dr^2}$ can be calculated analytically, even if the expressions are somewhat unwieldy. The integrals, on the other hand, are solved numerically, as there is no analytical master function for some integrals. Thus, a numerical recursion calculation was chosen in which an energy value was specified as a seed and converges with a relative accuracy $< 10^{-16}$. However, the condition for the calculation was the knowledge of r_e and thus f_E from (14), which were obviously not known at the beginning of this report. Nevertheless, they can be provided by the literature via l_P , if the electron is considered to be a quasi-point-like particle.

Consequently, the energy value $E_0 = -24.6\text{eV}$ taken from the literature was used to determine f_E and thus r_e backwards as a seed, like already mentioned in Chapter 4. This procedure proved the consistency of the calculation, because if we now apply $r_e = 3.4062 \cdot 10^{-36}\text{m} \approx l_P$ backwards, we arrive at the literature value for the ground state of the parahelium as described in the calculations. So given r_e with a physical plausible value one can reproduce the ground energy of helium. The Matlab script used here can be found in the appendix.

Now the question must be allowed as to why only the ground state of helium was evaluated in this report, while the hydrogen solution was able to derive the entire energy spectrum with all quantum states. The answer is of course obvious: the ground state of helium is exotic in the sense that the two electrons interact with each other to the maximum extent and f_E shows correspondingly the highest value – therefore the strongest effect. Moreover, due to this phenomenon the ground state of helium is not orthogonal to the higher excited states as in the hydrogen atom, which also makes a

closed formulation of the energy spectra much more difficult. An excited state of the helium atom such as $He^*(1s^0 2p^1)$ has a significantly lower overlap of the two electrons and thus a reduced exchange interaction while at the same time a lower correction factor for the vacuum polarization is necessary. This means that such a state can be described with acceptable accuracy by the superposition of two hydrogen states - as already described in the literature [11,12]. The smaller the overlap of the two electron wave functions is, the better is the approximation. This report thus closes to a certain extent the gap between the already well calculable excitation and ionization states and the various approximations via variational calculations from the literature for the ground state. Nevertheless, the method from Chapter 3 can of course also be used for perturbation calculations for the electron potentials.

8. Conclusion and outlook

In this report an analytical solution of the Schrodinger equation for neutral helium in the ground state was presented. Neither perturbation calculus nor variational methods are used, but the differential equation is solved directly using the Laplace transformation and the result is evaluated.

To enable these solutions, the nature of the closed shell and the properties of the wave function for both electrons are investigated. It was shown that both electrons occupy the identical quantum state and thus in consequence cover the same place at the same time. Another important step was to derive a general formula of an electron potential, to facilitate the potential term of the electron density function in the form of a radial probability density. This is accomplished by means of a convolution product of the Coulomb point-like potential with said squared wave function.

However, these measures show that an important element is still missing, because the identical quantum states bring the electrons very close together.

Quantum electrodynamics, in particular the Wichmann-Kroll potential, is used to illustrate the vacuum polarization effects for the consideration of energy at minimal distances. If an electron is understood as a Gaussian distributed structure and folded with the Wichmann-Kroll potential, the consequences are fascinating, because the result is a distance that exhibits a stable energy minimum, i.e., two electrons strongly approximated by external constraining forces exhibit a quasi-bonding state, albeit with a rather low binding energy, which only becomes significant in the mK range from a thermal point of view. Nevertheless, this indicates a quasi-bosonic entanglement state, which can also be associated with superfluidity effects. Last but not least, this approach makes it possible to estimate the geometric dimensions of the electron: It turns out that - for the analog of the Gauss curve - the 3σ width of the electron corresponds to the Planck length l_P , thus it could be shown that the electron can actually be understood as a point-like particle within the Planck scale. Finally, the correct coupling factor for the electron binding energy was determined and a mechanism could be shown that explains the robustness of helium against perturbations plausibly - such as chemical inertness - based on quantum electrodynamic effects, i.e., it can explain the physical phenomenon of the closed shell.

With this knowledge, the Schrodinger equation could now be solved analytically. The result is a wave function similar - but not the same - as the ground state of hydrogen, whereby the electrons are further away from the nucleus, but are significantly closer to the atomic nucleus overall due to the larger exponential spatial damping constant of the orbital. This creates the seemingly paradoxical impression of a larger "Bohr" distance with comparable atomic dimensions to hydrogen at the same time. The energy determination rounds off the report, whereby a recursive algorithm was used here, as the binding energy occurs intrinsically in the wave function and cannot be explicitly resolved. It

turns out that the literature value for the binding energy of helium can be reproduced with given values for l_P .

The method of folding a point potential with a spatially expanded charge opens a wide range of possibilities, whereby this report only makes a small contribution. Since geometrically finite structures are almost always found in nature, this method provides insights into the most diverse areas with surprising findings such as the geometric dimensioning of particles or the investigation of quantum electrodynamical effects. It seems promising to investigate further problems that are currently formulated with mathematically singular expressions and to check whether this method could possibly offer a way to a solution.

9. Annex

Chapter 4 referred to the fact, that every potential caused by electrons present in the vicinity of the atom can be modelled as a sum over n of a polynomial expression multiplied with an exponential damped probability depending on the distance to the core with the specific parameters A_n and a_n . It is now to prove, that this is as well the case for the derived wave function (29) in chapter 6. Now if one uses some reformulation of the equation (29) it is easy to find that:

$$\begin{aligned}
 R(r) &= f_N \frac{rsinh(\alpha r)}{\left(\frac{\alpha^2}{A}r + cosh(\alpha r)\right)^2} = 2f_N \frac{r(e^{\alpha r} - e^{-\alpha r})}{\left(\frac{2\alpha^2}{A}r + e^{\alpha r} + e^{-\alpha r}\right)^2} \\
 &= 2f_N r \left[\frac{e^{\alpha r}}{\left(\frac{2\alpha^2}{A}r + e^{\alpha r} + e^{-\alpha r}\right)^2} - \frac{e^{-\alpha r}}{\left(\frac{2\alpha^2}{A}r + e^{\alpha r} + e^{-\alpha r}\right)^2} \right] \\
 &= 2f_N r \left[\frac{e^{-\alpha r}}{\left(\frac{2\alpha^2}{A}re^{-\alpha r} + 1 + e^{-2\alpha r}\right)^2} - \frac{e^{-\alpha r}}{\left(\frac{2\alpha^2}{A}r + e^{\alpha r} + e^{-\alpha r}\right)^2} \right] \\
 &= 2f_N r e^{-\alpha r} \left[\sum_{n=0}^{\infty} \frac{\partial^n}{\partial r^n} \left\{ \left(\frac{2\alpha^2}{A}re^{-\alpha r} + 1 + e^{-2\alpha r} \right)^{-2} \right\} \right|_{r_0} \frac{(r - r_0)^n}{n!} \\
 &\quad - \sum_{n=0}^{\infty} \frac{\partial^n}{\partial r^n} \left\{ \left(\frac{2\alpha^2}{A}r + e^{\alpha r} + e^{-\alpha r} \right)^{-2} \right\} \right|_{r_0} \frac{(r - r_0)^n}{n!} \tag{33}
 \end{aligned}$$

Where one uses Taylor's formula to expand the function to a polynomial expression multiplied with exponential damped probability. The expansion is valid for every point over $\forall r \geq 0$ and converges as well for \mathbb{R}_0^+ . So, it is obvious to see that (33) is equivalent to the expression in (11) and that the approach to implement $R(r)$ into the Schrodinger equation is valid. Hence it is also proven, that (29) is a valid solution of the Schrodinger equation.

10. Bibliography

1. Hylleraas, E.A. and Undheim, B. (1930) 'Numerische Berechnung der 2S-Terme von Ortho- und Par-Helium', *Zeitschrift für Physik*, 65(11), pp. 759–772. Available at: <https://doi.org/10.1007/BF01397263>.
2. Bader, P. (1978) 'Variational method for the Hartree equation of the helium atom', *Proceedings of the Royal Society of Edinburgh Section A: Mathematics*, 82(1–2), pp. 27–39. Available at: <https://doi.org/10.1017/S030821050001101X>.
3. 8: The Helium Atom (2014) *Chemistry LibreTexts*. Available at: [https://chem.libretexts.org/Bookshelves/Physical_and_Theoretical_Chemistry_Textbook_Maps/Supplemental_Modules_\(Physical_and_Theoretical_Chemistry\)/Quantum_Mechanics/10%3A_Multi-electron_Atoms/8%3A_The_Helium_Atom](https://chem.libretexts.org/Bookshelves/Physical_and_Theoretical_Chemistry_Textbook_Maps/Supplemental_Modules_(Physical_and_Theoretical_Chemistry)/Quantum_Mechanics/10%3A_Multi-electron_Atoms/8%3A_The_Helium_Atom) (Accessed: 3 June 2024).
4. Doma, S.B. and El-Gammal, F.N. (2012a) 'Application of variational Monte Carlo method to the confined helium atom', *Journal of Theoretical and Applied Physics*, 6(1), p. 28. Available at: <https://doi.org/10.1186/2251-7235-6-28>.
5. Doma, S.B. and El-Gammal, F.N. (2012b) 'Application of variational Monte Carlo method to the confined helium atom', *Journal of Theoretical and Applied Physics*, 6(1), p. 28. Available at: <https://doi.org/10.1186/2251-7235-6-28>.
6. Drake, G.W. (1988) 'Theoretical energies for the n = 1 and 2 states of the helium isoelectronic sequence up to Z = 100', *Canadian Journal of Physics*, 66(7), pp. 586–611. Available at: <https://doi.org/10.1139/p88-100>.
7. Drake, G.W.F. and Yan, Z.-C. (1992) 'Energies and relativistic corrections for the Rydberg states of helium: Variational results and asymptotic analysis', *Physical Review A*, 46(5), pp. 2378–2409. Available at: <https://doi.org/10.1103/PhysRevA.46.2378>.
8. Dreizler, R.M. and Lüddecke, C.S. (eds) (2008) 'Das Helium Atom', in *Theoretische Physik: Band 3: Quantenmechanik 1*. Berlin, Heidelberg: Springer, pp. 329–350. Available at: https://doi.org/10.1007/978-3-540-48802-6_14.
9. Dushman, S. (1936) *Elements of the quantum theory. IX. The helium atom. Part II. The variational method*, ACS Publications. Division of Chemical Education. Available at: <https://doi.org/10.1021/ed013p179>.
10. Helium Energy Levels (no date). Available at: <http://hyperphysics.phy-astr.gsu.edu/hbase/quantum/helium.html> (Accessed: 3 June 2024).
11. Hertel, I.V. and Schulz, C.-P. (2017b) 'Helium und andere Zweielektronensysteme', in I.V. Hertel and C.-P. Schulz (eds) *Atome, Moleküle und optische Physik 1: Atome und Grundlagen ihrer*

Spektroskopie. Berlin, Heidelberg: Springer, pp. 375–411. Available at: https://doi.org/10.1007/978-3-662-53104-4_7.

12. Kinoshita, T. (1957) 'Ground State of the Helium Atom', *Physical Review*, 105(5), pp. 1490–1502. Available at: <https://doi.org/10.1103/PhysRev.105.1490>.

13. Lowy, D.N. and Woo, C.-W. (1976) 'New variational treatment of the ground state of solid helium', *Physical Review B*, 13(9), pp. 3790–3798. Available at: <https://doi.org/10.1103/PhysRevB.13.3790>.

14. Neumann, R. (1981) 'Helium and helium-like systems', in G. Gräff, E. Klempert, and G. Werth (eds) *Present Status and Aims of Quantum Electrodynamics*. Berlin/Heidelberg: Springer-Verlag (Lecture Notes in Physics), pp. 251–266. Available at: <https://doi.org/10.1007/BFb0033892>.

15. Pan, X.-Y., Sahni, V. and Massa, L. (2005) 'The constrained-search--variational method: application to the ground state of Helium atom'. arXiv. Available at: <https://doi.org/10.48550/arXiv.physics/0501107>.

16. 'Variational method for ground-state energy of helium atom in N dimensions' (2010) *Il Nuovo Cimento B*, 125(9), pp. 1099–1108. Available at: <https://doi.org/10.1393/ncb/i2010-10907-2>.

17. Banerjee, A., Kamal, C. and Chowdhury, A. (2006) 'Calculation of ground- and excited-state energies of confined helium atom', *Physics Letters A*, 350(1), pp. 121–125. Available at: <https://doi.org/10.1016/j.physleta.2005.10.024>.

18. Dyke, P. (2014) *An Introduction to Laplace Transforms and Fourier Series*. London: Springer (Springer Undergraduate Mathematics Series). Available at: <https://doi.org/10.1007/978-1-4471-6395-4>.

19. Edwards, R.E. (1979) 'Convolutions of Functions', in R.E. Edwards (ed.) *Fourier Series: A Modern Introduction Volume 1*. New York, NY: Springer, pp. 50–68. Available at: https://doi.org/10.1007/978-1-4612-6208-4_3.

20. Heil, C. (2019) 'Convolution and the Fourier Transform', in Heil, C., *Introduction to Real Analysis*. Cham: Springer International Publishing (Graduate Texts in Mathematics), pp. 327–386. Available at: https://doi.org/10.1007/978-3-030-26903-6_9.

21. Argeri, M. and Mastrolia, P. (2007) 'Feynman diagrams and differential equations', *International Journal of Modern Physics A*, 22(24), pp. 4375–4436. Available at: <https://doi.org/10.1142/S0217751X07037147>.

22. Dyson, F.J. (1949) 'The Radiation Theories of Tomonaga, Schwinger, and Feynman', *Physical Review*, 75(3), pp. 486–502. Available at: <https://doi.org/10.1103/PhysRev.75.486>.

23. Fainshtein, A.G., Manakov, N.L. and Nekipelov, A.A. (1991) 'Vacuum polarization by a Coulomb field. Analytical approximation of the polarization potential', *Journal of Physics B: Atomic, Molecular and Optical Physics*, 24(3), p. 559. Available at: <https://doi.org/10.1088/0953-4075/24/3/012>.
24. Frolov, A.M. (2021) 'Uehling potential and lowest-order corrections on vacuum polarization to the cross sections of some QED processes', *The European Physical Journal A*, 57(2), p. 79. Available at: <https://doi.org/10.1140/epja/s10050-021-00394-y>.
25. Frolov, A.M. and Wardlaw, D.M. (2012) 'Analytical formula for the Uehling potential', *The European Physical Journal B*, 85(10), p. 348. Available at: <https://doi.org/10.1140/epjb/e2012-30408-4>.
26. Frolov, A.M. and Wardlaw, D.M. (2014) 'Vacuum polarization in light two-electron atoms and ions', *Journal of Computational Science*, 5(3), pp. 499–506. Available at: <https://doi.org/10.1016/j.jocs.2013.03.005>.
27. Huang, K.-N. (1976) 'Calculation of the vacuum-polarization potential', *Physical Review A*, 14(4), pp. 1311–1318. Available at: <https://doi.org/10.1103/PhysRevA.14.1311>.
28. Klingbeil, H. (2022) 'Klassifikation feldtheoretischer Probleme und Potentialansätze', in H. Klingbeil (ed.) *Grundlagen der elektromagnetischen Feldtheorie : Maxwellgleichungen, Lösungsmethoden und Anwendungen*. Berlin, Heidelberg: Springer, pp. 153–217. Available at: https://doi.org/10.1007/978-3-662-65126-1_4.
29. Mayer-Kuckuk, T. (2013a) *Atomphysik: Eine Einführung*. Springer-Verlag. Available at: https://books.google.com/books?hl=de&lr=&id=XNwk-BgAAQBAJ&oi=fnd&pg=PA9&dq=mayer+kuckuk&ots=Bc9Tx5zEfW&sig=RZSzzzYG0in-QECEBWITQK18m_KU (Accessed: 30 October 2023).
30. Mayer-Kuckuk, T. (2013b) *Kernphysik: Eine Einführung*. Springer-Verlag. Available at: <https://books.google.com/books?hl=de&lr=&id=nJUiB-gAAQBAJ&oi=fnd&pg=PA9&dq=mayer+kuckuk&ots=344YpsVEqb&sig=D0Qn7Bylq2N0UO99JmG-m4Wz10g> (Accessed: 30 October 2023).
31. Wichmann, E.H. and Kroll, N.M. (1956) 'Vacuum Polarization in a Strong Coulomb Field', *Physical Review*, 101(2), pp. 843–859. Available at: <https://doi.org/10.1103/PhysRev.101.843>.
32. Persson, H. et al. (1993) 'Accurate vacuum-polarization calculations', *Physical Review A*, 48(4), pp. 2772–2778. Available at: <https://doi.org/10.1103/PhysRevA.48.2772>.
33. Ehlotzky, F. (ed.) (2005) 'Systeme mehrerer Teilchen', in *Quantenmechanik und ihre Anwendungen*. Berlin, Heidelberg: Springer (Springer-Lehrbuch), pp. 195–222. Available at: https://doi.org/10.1007/3-540-26754-9_8.

34. Frolov, A.M. (2013) 'On the properties of the Uehling potential'. arXiv. Available at: <https://doi.org/10.48550/arXiv.1210.6737>.
35. Frolov, A.M. (2014) 'On the interaction between two point electric charges', *Canadian Journal of Physics*, 92(10), pp. 1094–1101. Available at: <https://doi.org/10.1139/cjp-2013-0533>.
36. Nolting, W. (1997) *Grundkurs Theoretische Physik 5 Quantenmechanik*. Wiesbaden: Vie-weg+Teubner Verlag. Available at: <https://doi.org/10.1007/978-3-663-14691-9>.
37. Schwabl, F. (2007) *Quantenmechanik (QM I): Eine Einführung*. Springer-Verlag. Available at: <https://books.google.com/books?hl=de&lr=&id=DPwdBAAQBAJ&oi=fnd&pg=PA1&dq=schwabl+quantenmechanik&ots=P5W0cSQpYB&sig=ijCCI0VVk4DTV6kfIhIJ3IJAbCE> (Accessed: 30 October 2023).
38. Schwabl, F. (2008) *Quantenmechanik für Fortgeschrittene (qm ii)*. Springer-Verlag. Available at: <https://books.google.com/books?hl=de&lr=&id=KPln-BAAQBAJ&oi=fnd&pg=PA3&dq=schwabl+quantenmechanik&ots=SY0LqzBE1&sig=Ph8s8Png9qPhTJweTOHgCCswpko> (Accessed: 30 October 2023).
39. Wachter, A. (2006) *Relativistische Quantenmechanik*. Springer-Verlag. Available at: <https://books.google.com/books?hl=de&lr=&id=MocfBAAQBAJ&oi=fnd&pg=PR14&dq=relativistische+quantenmechanik&ots=ebNCnTE95I&sig=1Sxw0JnZ45ewmgdsT-M3f7519fI> (Accessed: 30 October 2023).
40. Wachter, A. (2010) 'Relativistic Description of Spin-1/2 Particles', in Wachter, A., *Relativistic Quantum Mechanics*. Dordrecht: Springer Netherlands (Theoretical and Mathematical Physics), pp. 85–176. Available at: https://doi.org/10.1007/978-90-481-3645-2_2.
41. Wolschin, G. (2021) *Relativistische Quantenmechanik*. Berlin, Heidelberg: Springer Berlin Heidelberg. Available at: <https://doi.org/10.1007/978-3-662-64387-7>.
42. Berker, A.N. and Nelson, D.R. (1979) 'Superfluidity and phase separation in helium films', *Physical Review B*, 19(5), pp. 2488–2503. Available at: <https://doi.org/10.1103/PhysRevB.19.2488>.
43. Donnelly, R.J. (2009) 'The two-fluid theory and second sound in liquid helium', *Physics Today*, 62(10), pp. 34–39. Available at: <https://doi.org/10.1063/1.3248499>.
44. Fetter, A.L. (1967) 'Quantum Theory of Superfluid Vortices. I. Liquid Helium II', *Physical Review*, 162(1), pp. 143–153. Available at: <https://doi.org/10.1103/PhysRev.162.143>.
45. Fiedler, S.L. and Eloranta, J. (2014) 'Interaction of Helium Rydberg State Atoms with Superfluid Helium', *Journal of Low Temperature Physics*, 174(5), pp. 269–283. Available at: <https://doi.org/10.1007/s10909-013-0991-6>.

46. Ancilotto, F. *et al.* (2017) 'Density functional theory of doped superfluid liquid helium and nanodroplets', *International Reviews in Physical Chemistry*, 36(4), pp. 621–707. Available at: <https://doi.org/10.1080/0144235X.2017.1351672>.
47. Jaishy, B. (2015) 'THEORY OF SUPERFLUIDITY IN HELIUM- A REVIEW', *Journal of Applied and Fundamental Sciences*, 1(2), p. 160.
48. Pandolfi, L. (no date) 'The Lebesgue Integral Via The Tonelli Method'.
49. 'Real Analysis MAA 6616 Lecture 18 Tonelli's Theorem and Applications' (no date).
50. Wolf, D. (1999) *Signaltheorie*. Berlin, Heidelberg: Springer Berlin Heidelberg. Available at: <https://doi.org/10.1007/978-3-642-58540-1>.
51. Yoshizawa, H. (1954) 'A Proof of the Plancherel Theorem', *Proceedings of the Japan Academy*, 30(4), pp. 276–281. Available at: <https://doi.org/10.3792/pja/1195526107>.
52. *A Proof of the Plancherel Theorem* (no date). Available at: https://www.jstage.jst.go.jp/article/pjab1945/30/4/30_4_276/_article/-char/ja/ (Accessed: 3 June 2024).
53. *Advanced Analysis* (no date). Available at: <https://www2.math.upenn.edu/~gressman/analysis/14-plancherel.html> (Accessed: 3 June 2024).
54. Weisstein, E.W. (no date) *Plancherel's Theorem*. Wolfram Research, Inc. Available at: <https://mathworld.wolfram.com/> (Accessed: 3 June 2024).
55. Asher, K. (2013) 'An Introduction to Laplace Transform', 2(1).
56. Doetsch, G. (2012) *Introduction to the Theory and Application of the Laplace Transformation*. Springer Science & Business Media.
57. Doetsch, G. (2013) *Theorie und Anwendung der Laplace-Transformation*. Springer-Verlag.
58. Edmonds, S.M. (1947) 'The Parseval formulae for monotonic functions. I', *Mathematical Proceedings of the Cambridge Philosophical Society*, 43(3), pp. 289–306. Available at: <https://doi.org/10.1017/S0305004100023525>.
59. Hackbusch, W. *et al.* (2012) *Springer-Taschenbuch der Mathematik: Begründet von IN Bronstein und KA Semendjaew Weitergeführt von G. Grosche, V. Ziegler und D. Ziegler Herausgegeben von E. Zeidler*. Springer-Verlag. Available at: <https://books.google.com/books?hl=de&lr=&id=6TMgBAAQBAJ&oi=fnd&pg=PR5&dq=Taschenbuch+der+Mathematik&ots=vRAoaoCjbB&sig=HOfRMpUvCyV7U2TCEVo5ywZWuBY> (Accessed: 30 October 2023).
60. Jafari, H. (2021) 'A new general integral transform for solving integral equations', *Journal of Advanced Research*, 32, pp. 133–138. Available at: <https://doi.org/10.1016/j.jare.2020.08.016>.
61. *Laplace - Transformation | SpringerLink* (no date). Available at: https://link.springer.com/chapter/10.1007/978-3-8351-9104-4_4 (Accessed: 2 June 2024).

62. *mathe online skripten laplace transformation at DuckDuckGo* (no date). Available at: <https://duckduckgo.com/?hps=1&q=mathe+online+skripten+laplace+transformation&atb=v280-1&ia=web> (Accessed: 2 June 2024).

63. Oberhettinger, F. and Badii, L. (2012) *Tables of Laplace Transforms*. Springer Science & Business Media.

64. *Atomic Radii* (2013) *Chemistry LibreTexts*. Available at: [https://chem.libretexts.org/Bookshelves/Physical_and_Theoretical_Chemistry_Textbook_Maps/Supplemental_Modules_\(Physical_and_Theoretical_Chemistry\)/Physical_Properties_of_Matter/Atomic_and_Molecular_Properties/Atomic_Radii](https://chem.libretexts.org/Bookshelves/Physical_and_Theoretical_Chemistry_Textbook_Maps/Supplemental_Modules_(Physical_and_Theoretical_Chemistry)/Physical_Properties_of_Matter/Atomic_and_Molecular_Properties/Atomic_Radii) (Accessed: 3 June 2024).

65. *Atomic Radius for all the elements in the Periodic Table* (no date). Available at: <https://periodictable.com/Properties/A/AtomicRadius.v.html> (Accessed: 3 June 2024).

66. Finkelburg, W. (2013a) *Einführung in die Atomphysik*. Springer-Verlag. Available at: https://books.google.com/books?hl=de&lr=&id=2b2oBgAAQBAJ&oi=fnd&pg=PA1&dq=atomphysik&ots=zz0r7gN8uS&sig=SaoYEe5J2dDFOO_XxAAMDzuJNs (Accessed: 31 October 2023).

67. Finkelburg, W. (2013b) *Einführung in die Atomphysik*. Springer-Verlag.

68. Ghosh, D.C. and Biswas, R. (2002) 'Theoretical Calculation of Absolute Radii of Atoms and Ions. Part 1. The Atomic Radii', *International Journal of Molecular Sciences*, 3(2), pp. 87–113. Available at: <https://doi.org/10.3390/i3020087>.

69. Ohayon, B. *et al.* (2023) 'Towards Precision Muonic X-Ray Measurements of Charge Radii of Light Nuclei'. arXiv. Available at: <https://doi.org/10.48550/arXiv.2310.03846>.

70. Ozawa, A. (2020) 'Matter Radii and Density Distributions', in I. Tanihata, H. Toki, and T. Kajino (eds) *Handbook of Nuclear Physics*. Singapore: Springer Nature, pp. 1–26. Available at: https://doi.org/10.1007/978-981-15-8818-1_40-1.

71. Ozawa, A. (2023) 'Matter Radii and Density Distributions', in I. Tanihata, H. Toki, and T. Kajino (eds) *Handbook of Nuclear Physics*. Singapore: Springer Nature, pp. 217–242. Available at: https://doi.org/10.1007/978-981-19-6345-2_40.

72. PubChem (no date) *Atomic Radius / Periodic Table of Elements*. Available at: <https://pubchem.ncbi.nlm.nih.gov/periodic-table/atomic-radius> (Accessed: 3 June 2024).

73. Bearden, J.A. and Burr, A.F. (1967) 'Reevaluation of X-Ray Atomic Energy Levels', *Reviews of Modern Physics*, 39(1), pp. 125–142. Available at: <https://doi.org/10.1103/RevModPhys.39.125>.

74. 'Bindungsenergie' (2023) *Wikipedia*. Available at: <https://de.wikipedia.org/w/index.php?title=Bindungsenergie&oldid=237089826> (Accessed: 4 November 2023).

75. Cardona, M. and Ley, L. (1978) *Photoemission in solids I*. Available at: <https://ui.adsabs.harvard.edu/abs/1978ps1..book....C/abstract> (Accessed: 30 October 2023).
76. Guenault, T. (2002) *Basic Superfluids*. CRC Press.
77. Porter, F.T. and Freedman, M.S. (1978) 'Recommended atomic electron binding energies, 1 s to 6 p 3/2, for the heavy elements, Z = 84 to 103', *Journal of Physical and Chemical Reference Data*, 7(4), pp. 1267–1284. Available at: <https://doi.org/10.1063/1.555584>.

11. Matlab-Code for numerical calculations

```

clear all
close all
clc
tic;
syms x;
% Definiere die Konstanten
PI = sym(pi);
hquer = sym(6.62607015e-34)/(sym(2)*PI); % Js
C = sym(299792458); % m/s
e_e = sym(1.602176634e-19); % Elementarladung in Coulomb
m_e = sym(9.1093837015e-31); % kg -> Elektronenmasse
m_P = sym(1.67262192369e-27); % kg -> Protonenmasse
r_P = sym(0.8409e-15); % Protonenradius in m
m_N = sym(1.67492749804e-27); % kg -> Neutronenmasse
Epsilon0 = sym(8.8541878128e-12); % A*s/(V*m)
Atommasse = sym(4); % 
Z_Ladung = sym(2); % Ladungszahl des Kerns, hier Pb203
m_e_red = m_e/(1+ m_e/(Z_Ladung*m_P+(Atommasse-Z_Ladung)*m_N)); % Berechne die reduzierte Masse des Elektrons
% Zur Vereinfachung
% Ebenfalls zur Erleichterung
% Sommerfeldsche Feinstrukturkonstante
% Ruheenergie des Elektrons
% Bindungsenergie des Protons
% Bindungsenergie für Wasserstoff
K_1 = Z_Ladung * e_e^2 / (4 * PI * Epsilon0);
K_2 = hquer^2/(2*m_e_red);
K_alpha = e_e^2 / (4 * PI * Epsilon0 * hquer * C);
E_0 = m_e*C.^2;
E_Proton = sym(8.0e6)*e_e;
E_H = e_e^sym(4)*m_e/(sym(8)*Epsilon0^2*(hquer^2*PI)^2);
Compton_WL = sym(hquer/m_e/C);
G = sym(6.67430e-11);
% Funktionen zur Berechnung definieren
A = Z_Ladung * sym(2) * m_e * e_e^2 / (sym(4) * PI * Epsilon0 * hquer^2);
B = sym(2) * m_e / hquer^2;
C_C = B * e_e^2 / (sym(4) * PI * Epsilon0)* 1/(sym(2)*sqrt(sym(2)*PI));
E_seed = sym(-24.6*e_e);
test = sym(0);
l_P = sqrt(hquer*G/C^3);
threshold = sym(1e-16);
scale_factor = sym(1);%sym(1.264468);
while (abs((scale_factor-test)/scale_factor)>threshold)
    if test ~= 0
        scale_factor=test;
    end
    r_e = l_P/6 * scale_factor;
    a_min = sym(1.10628);
    factor = double(1 - (sym(4)*Epsilon0)*sqrt(2)*hquer*e_e^8/(675*m_e^4*C^7*(4*PI)^4*r_e^4).*(3 - 12*a_min^2 + 4*a_min^4).*exp(-a_min^2));
    alpha = sqrt(factor * C_C/sqrt(sym(2)*PI) - B * sym(E_seed));
    R(x) = x/alpha * sinh(x)/(alpha/A*x + cosh(x))^2;
    dR_dx(x) = diff(R);
    ddR_dx(x) = diff(dR_dx);
    f_N_R = sym(1) / vpaintegral(x^2*R^2,0,inf);
    E_1 = + alpha^2 * vpaintegral(x^2*R*ddR_dx(x),0,inf);
    E_2 = + sym(2) * alpha^2 * vpaintegral(x*R*ddR_dx(x),0,inf);
    E_3 = + A * alpha * vpaintegral(x^2,0,inf);
    E_4 = - f_N_R * sym(2) * factor * C_C * alpha * vpaintegral(x^4*R^4,0,inf);
    E_result = (f_N_R * (E_1 + E_2 + E_3 + E_4) / B);
    test = test - (E_seed - E_result)/E_seed/5;
    fprintf('scale_factor = %3.2f\n',double(scale_factor));
    fprintf('relative error = %3.2f *1e-18\n\n',double((E_result-E_seed)/E_seed)*1e16);
end
dsf = double(scale_factor);
toc

```